Hindawi
Advances in Materials Science and Engineering
Volume 2022, Article ID 5249999, 11 pages
https://doi.org/10.1155/2022/5249999

Research Article

Frost Heaving Properties of Gravelly Soils in Alpine Seasonally Frozen Regions

Cheng Chen,[1] Zhigang Zhang,[1] Li Ling,[1] Baoyuan He,[1] Yanjia Jiang,[2] and Zhihe Cheng[2]

[1]*State Grid East Inner Mongolia Electric Power Company Limited, Hohhot 150100, China*
[2]*School of Civil Engineering, Harbin Institute of Technology, Harbin 150090, China*

Correspondence should be addressed to Zhihe Cheng; 17204054005@stu.xust.edu.cn

Received 22 July 2022; Revised 23 August 2022; Accepted 31 August 2022; Published 10 September 2022

Academic Editor: Quantao Liu

To investigate the frost heaving properties of gravelly soil in alpine seasonally frozen regions and provide a foundation for the antifrost heaving design of the foundation tower in the Manzhouli 500 kV electrical transmission line. First, particle analysis and compaction tests were used to assess the basic characteristics of gravelly soil. Then, to investigate, a unidirectional freezing test of graded sand was performed to analyze the regularity and properties of the frozen process of graded sand. The test results demonstrate that the temperature gradient and the number of freeze-thaw cycles considerably affect the freezing of graded sand. The greater the temperature gradient and the number of freeze-thaw cycles, the greater the frost heave. In the freezing process, graded sand with zero fine-grain content exhibits obvious freezing shrinkage and thawing settlement. Still, the frost heave of sand is small. The frozen damage of graded sand is not caused by frost heaving deformation but by the deterioration of soil structure and the decrease of bearing capacity under hydrothermal coupling. Finally, experimental research is used to propose prevention and control measures for frost heave of power transmission and transformation projects.

1. Introduction

The frost heave effect of soil occurs primarily in permafrost with a high fine content during the construction and operation of projects in cold regions. Under the joint action of freezing temperature and water, ice crystals form in the ground, which causes deformation of soil surfaces, such as uplift, foundation uplift, and melting settlement [1]. They may even result in severe freezing damage due to engineering failure. Freezing damage is a hydro-thermo-mechanical coupled process, induced by the cycling load of pore ice pore pressure and thermal stress under hydro-thermo-mechanical conditions at low temperatures [2]. In order to clarify the mechanism of the coupling process, many scholars have conducted lots of research. Zhu et al. considered the effects of wetting-drying-freezing cycles on the mechanical behaviors of expansive soil by triaxial tests, and the research results can predict the stress-strain behavior [3]. Li et al. built a numerical water, thermal, and stress-coupled model based on energy, mass, and momentum conservation principles; the study is conducive to better explaining the interaction between water, temperature, and deformation and the frost heave mechanism of the freezing soil [4]. Li et al. used the split Hopkinson pressure bar device to evaluate the dynamic mechanical properties of frozen soil at different test conditions, constructing a viscoelastic-plastic constitutive model with damage of frozen soil [5].

Graded coarse-grained soil filler is typically considered frost-free as an essential engineering material in engineering construction. Nonetheless, in actual engineering, freezing damage caused by fillers often occurs. Fine particles in coarse packing change the frost heaving performance and weaken the bearing capacity, posing potential risks to the project's operation and maintenance. Therefore, it is critical to investigate the frost heaving performance of graded coarse-grained soil, considering the influence of the fine-grain content of engineering construction in permafrost areas. Everett proposed the capillary theory, which explained and estimated frost heave and frost heave force, but failed to explain the formation of discontinuous ice lenses and

underestimated the frost heave pressure in fine-grained soils [6]. Recognizing the shortcomings of the capillary theory, Tong et al. proposed a rigid ice model that includes an area where ice and water coexist between the bottom surface of the warmest ice and the freezing front [7]. Cheng and Deng discovered a relationship between different ice potentials and the frost heaving rate of coarse-grained soil by studying the particle size, and he concluded that the smaller the particle size, the stronger the effect [8]. Wang et al. conducted a lot of freezing tests of unsaturated soil, considering the influence of fine content and degree of saturation [9]. Geng et al. examined coarse aggregate differently and discovered that the coagulation potential decreased with the gradual increase in porosity of coarse aggregate and confirmed that the coagulation potential should be considered because of fine-grain content [10]. Tang et al. proposed that the range of fine soil and freezing conditions have the greatest influence on the frost heave sensitivity of water-saturated sand and gravel during freezing [11]. Ling et al. investigated the frost heaving properties of fine gravelly soil fillers, varying fine soil contents, and dry densities using Faustian compaction and frost heaving tests [12]. Wang and Yue studied the frost heave characteristics of Yanji expansive soil and proposed a coupled hydro-thermo-deformation frost heave model to research the frost heave deformation and expansive deformation of the soil [13]. Ju investigated the frost heaving rate and frost heaving characteristics of white sandstone soil through laboratory tests [14]. Guo et al. carried out a series of frost heaving simulation tests in a closed system for five coarse-grained soils with different soil materials under additional water content, saturation, and density conditions [15]. Jiang described the high and low temperature performance, fatigue performance, and moisture susceptibility of asphalt mixtures with aging [16].

In conclusion, frost heaving experimental research is carried out to explore the frost heaving deformation of graded soil during freezing, considering the influence of fine-grain content on the frost heaving law of graded coarse-grained soil, based on compaction degree, temperature conditions, freeze-thaw cycle, and water filling conditions, combined with appropriate monitoring means. This study investigated the development law of the frost heaving deformation of graded coarse-grained soil considering the influence of fine-grain content in the freezing region of the alpine season by monitoring the temperature field and deformation field in real time based on the indoor frost heaving test (See as shown in Table1).

2. Test

2.1. Particle Size Distribution and Soil Sample Preparation. The power transmission and transformation project are situated in a seasonally frozen high-latitude region. The main geological condition of the tower is fine sand. According to the specification of Standard Practice for Classification of Soils for Engineering Purposes (Unified Soil Classification System) (ASTM D2487-2017), the experiment was carried out by adding fine foreign particles with additional fine particle content to investigate the effect of different fine particle content on the basic physical properties and frost heaving effect of graded sand. The sand used in the test is from the Harbin Songhua River. Firstly, it is screened by particle size, as shown in Table 2. In cold weather, the mass fraction of particles with a diameter of less than 0.075 mm in sandy and gravelly soil is 1.84%. Then, four types of graded fine sand with different fine-grain content were prepared in proportion, with the fine-grain content being 0%, 5%, 10%, and 15%, respectively, represented as SF0, SF5, SF10, and SF15. Among them, 1250 mesh fine ground kaolin is used for fine particles. One is for the four gradations of sand particles, and Figure 1 is for the gradation curve. According to the grain gradation curve of graded sand, the nonuniformity coefficient Cu and the curvature coefficient Cc are calculated. Figure 2 depicts the calculation results. The nonuniformity coefficients of the four graded sands are 3.40, 3.35, 3.43, and 3.12, respectively, and the curvature coefficients are 0.65, 0.66, 0.68, and 0.63, according to the analysis.

2.2. Compaction Test. Standard compaction tests of gravelly soil with 0%, 5%, 10%, and 15% fine-grain content were performed to obtain the maximum dry density and optimal water content of sand and gravelly soil with different fine-grain content, as depicted in Figure 3. The full dry density moisture content of SF0, SF5, SF10, and SF15 ranges from 13% to 15%, and the maximum dry density ranges from 1.70 to 1.87 g/cm^3. The maximum dry density of fine sand gradually increases with increasing fine-grain content, as does the change interval of dry density in the experiment.

2.3. Frost Heave Test. To analyze the frost heaving effect of graded sand, a self-made one-dimensional freeze-thaw cycle system under open conditions was adopted. As shown in Figure 4, it is primarily composed of three components: a constant temperature control system, a water supply system, and a data acquisition system.

2.3.1. Constant Temperature Control System. The thermostatic control system comprises cold and warm end components, a thermostatic control device, and a cold bath cycle device. The cold and warm ends are made of copper disks with high thermal conductivity, and the hard bath circulation device uses anhydrous ethanol as the circulating liquid. The temperature range is +90°C~−30°C, and the control accuracy is ±0.1°C. The cold bath circulation device can regulate the temperature of the cold and warm ends as well as the ambient temperature.

2.3.2. Water Supply System. The system is pressure-free automatic water replenishment, and the Mars water bottle can eliminate the influence of gravity on water replenishment. Figure 5 depicts the working principle of Mohs filling water bottles.

Table 1: Natural frequency of two test models.

Category	Grain size (mm)	5	2	1	0.5	0.25	0.075
SF0	<Mass percentage of grain size (%)	100	90	85	70	55	0
SF5		100	90.5	85.75	71.5	57.25	5
SF10		100	91	86.5	73	59.5	10
SF15		100	91.5	87.25	74.5	61.75	15

Table 2: Boundary conditions of temperature water refill.

Serial number	Time (h)	H_c (°C)	H_h (°C)	Filling water valve	Note
1	0	3	3	Open	Constant temperature for 24 h
2	24	−3	3	Open	Freeze 8th
3	32	−12	0	Close	Frozen for 16 h
4	48	12	3	Open	Thawed for 16 h
5	64	3	3	Open	Constant temperature for 8th
6	72	−3	3	Open	Freeze 8th
7	80	−12	0	Close	Frozen for 16 h
8	96	12	3	Open	Thawed for 16 h

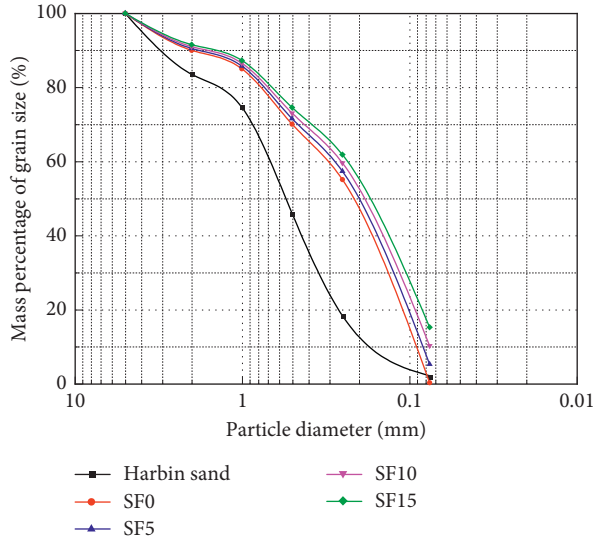

Figure 1: Grain gradation curves of four kinds of sand.

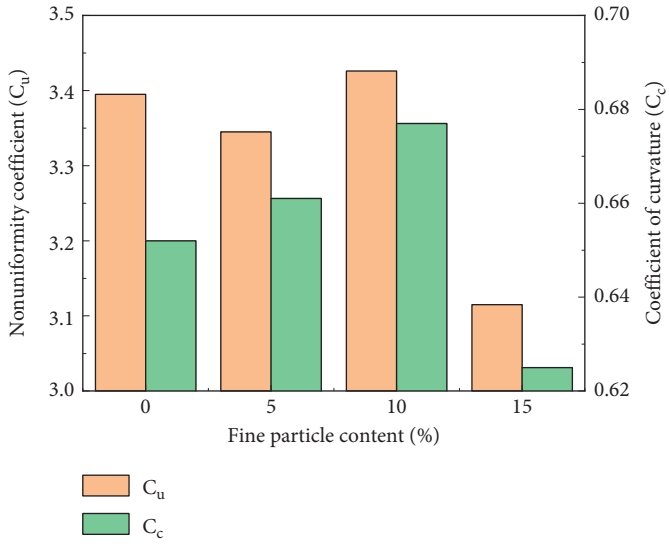

Figure 2: Cu and Cc plots of four sandy soils.

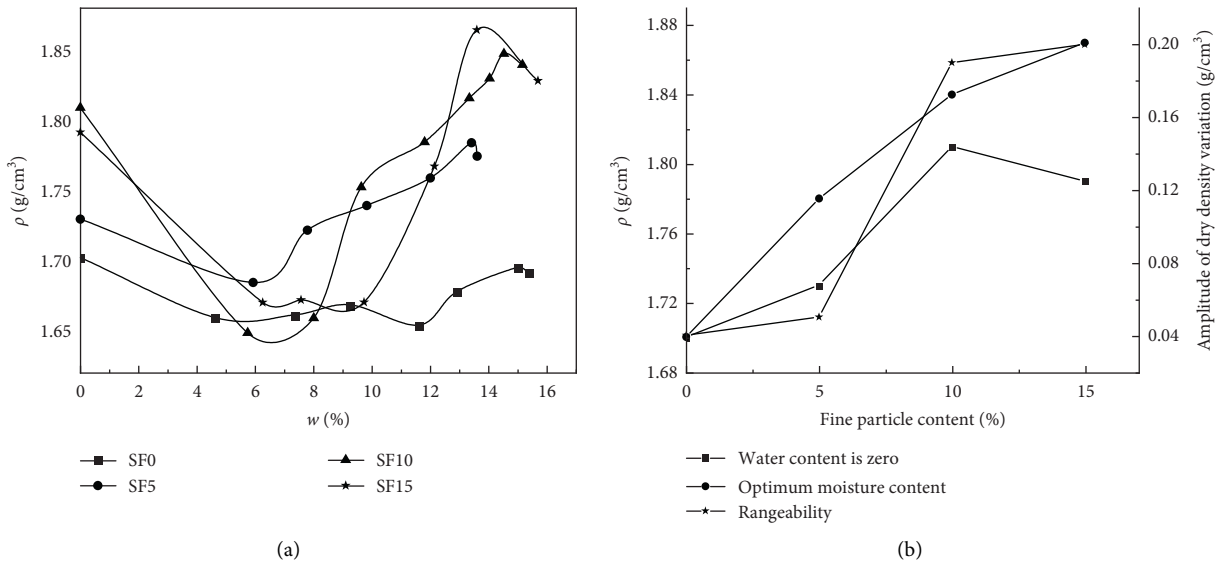

Figure 3: Compaction curves of four sandy soils and their variation amplitude of dry density: (a) compaction curve; (b) dry density and its increase.

Figure 4: Freezing test instrument: (a) free-thaw cycle equipment; (b) water supply system.

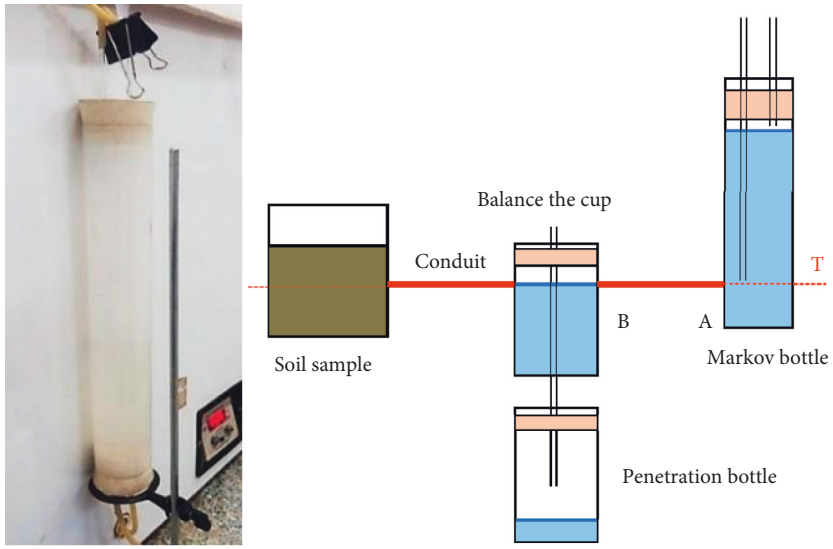

Figure 5: Schematic diagram of the water replenishment system.

2.3.3. Data Acquisition System. The data collection system's main components include a computer, sensor, and data acquisition instrument. The collection instrument can accurately measure and record the voltage, current, and resistance setting time intervals simultaneously. Sensor types mainly include temperature and displacement. The temperature sensor uses a needle sensor with a thermistor working principle, measuring a temperature range from 150°C to −50°C. The displacement sensor operates on a linear differential transformer sensor with a temperature range of 70°C~−20°C, and it is used to measure and record the displacement of frost heaving deformation at the top of the soil.

During the test, the cold, warm, and ambient temperatures were adjusted according to the test temperature and water refill boundary conditions provided by ASTM, as shown in Table 2. The purpose of the frost heaving test is to investigate the effect of a temperature gradient, several freeze-thaw cycles, and other factors on the temperature field, water field, water filling condition, frost heaving amount, and frost heaving rate of graded sand during the freezing process.

According to the temperature and water refill boundary conditions specified in Table 2, two freeze-thaw cycle tests were performed on graded sand. Each test included four stages of constant temperature, freezing for eighth, freezing for 16 h, and melting for 16 h, respectively (A1, B1: constant temperature stage; A2, B2: freezing the eighth stage; A3, B3: freezing stage for 16 h; A4, B4: melting stage), and the freezing test process is shown in Figure 6.

3. Test Results and Analysis

3.1. Temperature Field. The temperature change with time at each position of graded sand was recorded using a temperature sensor placed in the sample during the two freeze-thaw cycles. After sorting, the temperature change curve with time was drawn, as shown in Figure 7. Each test contained four separate phases: constant temperature, freezing for eighth, freezing for 16 h, and thawing for 16 h (A1, B1: constant temperature phase; A2, B2: freezing for eight h phase; A3, B3: freezing for 16 h phase; A4, B4: thawing phase). The figure shows that when freezing begins, the temperature begins to drop everywhere, with the cold end experiencing the greatest temperature drop. The farther away from the cold end, the lower the temperature drop rate. By comparing 8 h of starting freezing to 16 h of complete freezing, the temperature gradient has a direct influence on the development speed and freezing depth of the freezing front (A2 and A3 and B2 and B3). When the temperature field distributions of the two freeze-thaw cycles are compared, it is discovered that the freeze-thaw cycle has little effect on the temperature field distribution of graded sands during freezing [17–20].

3.2. Water Field. For the water content measurement test, the sample section was divided into 10 layers, with 2 layers about 1.5 cm from each layer. The final test results are shown in Figure 8. The figure shows that after the freezing test, the water content distribution decreases from 21.98% at the cold end to 17.54% at the warm end. The water content in the middle part fluctuates around 20% from 3 to 12 cm. Water migration occurred in the sand samples during the freezing process, and the migration was from the warm end to the cold end.

3.3. Frost Heave Response of Graded Sand. The variation value of the top displacement of the graded sand sample with time in the two freeze-thaw cycles was recorded using the displacement sensor arranged at the cold end of the top of the sample, and the curve of the freezing-heaving amount with time was drawn after arrangement, as shown in Figure 9. The findings are summarized as follows:

(1) The frost heaving rate and amount of graded sand increase with the temperature gradient increase

(2) In the freeze-thaw process, there is freezing shrinkage and thawing settlement of graded sand, the degree of which is directly affected by temperature gradients

(3) With the increase in the number of freeze-thaw cycles, the freezing shrinkage of graded sand decreases, and the amount of frost heave increases

(4) Overall, the frost heave of graded sand is very small, and the frost heaving rate is very low

The analysis of the A2, A3, B2, and B3 stages, as well as the study of the freezing process of graded sand samples, shows that the variation trend of frost heave of graded sand samples during the freezing process roughly conforms to the four development stages.

Step 1 (rapid growth): frost heave increases rapidly due to applying a freezing temperature gradient. Due to the intense ice separation during the soil freezing process, the frost heave of graded sand soil is rapidly rising, and thus the frost heaving deformation of sand soil is rapidly increasing.

Step 2 (slow growth): with the passage of freezing time, the frost heaving rate of graded sand decreases gradually, and frost heaving increases slowly. It could be due to the slow growth of ice lens thickness and the slow formation of new ice lenses, which causes the growth rate of graded sand frost heave to slow.

Step 3 (relatively stable): in this stage, the frost heaving rate of sand is close to zero. The frost heaving rate range is much smaller than that of stages 1 and 2, though the measurement voltage instability may cause minor fluctuations. It may be owing to a temporary equilibrium, but it does not last long.

Step 4 (frost heave and contraction): the frost heaving amount of graded sand begins to freeze and shrink from its stable state, which may be due to the structure of graded sand being damaged after freezing and its bearing capacity decreasing to the point where it is insufficient to support the ice pressure and overburden

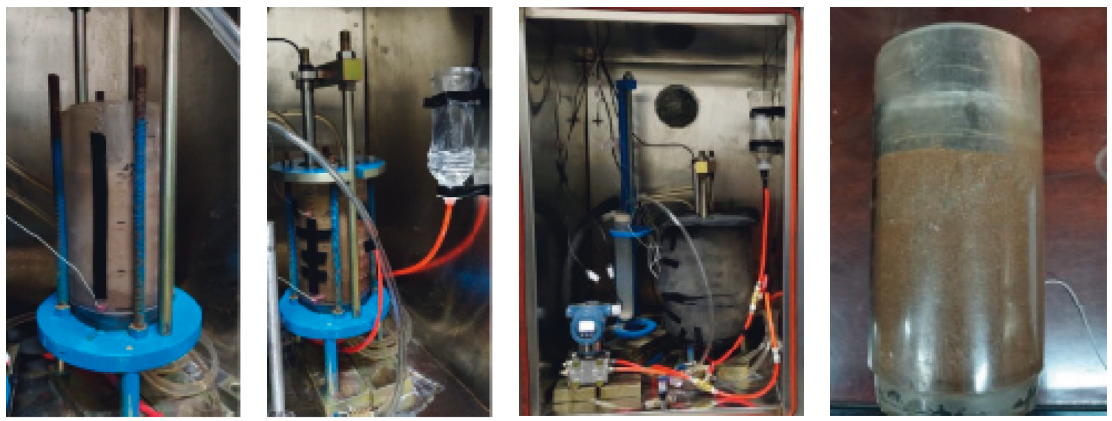

(a) (b) (c) (d)

Figure 6: Freezing process: (a) install the sample; (b) install refill water bottle; (c) install thermal insulation board materials; (d) remove sample barrel.

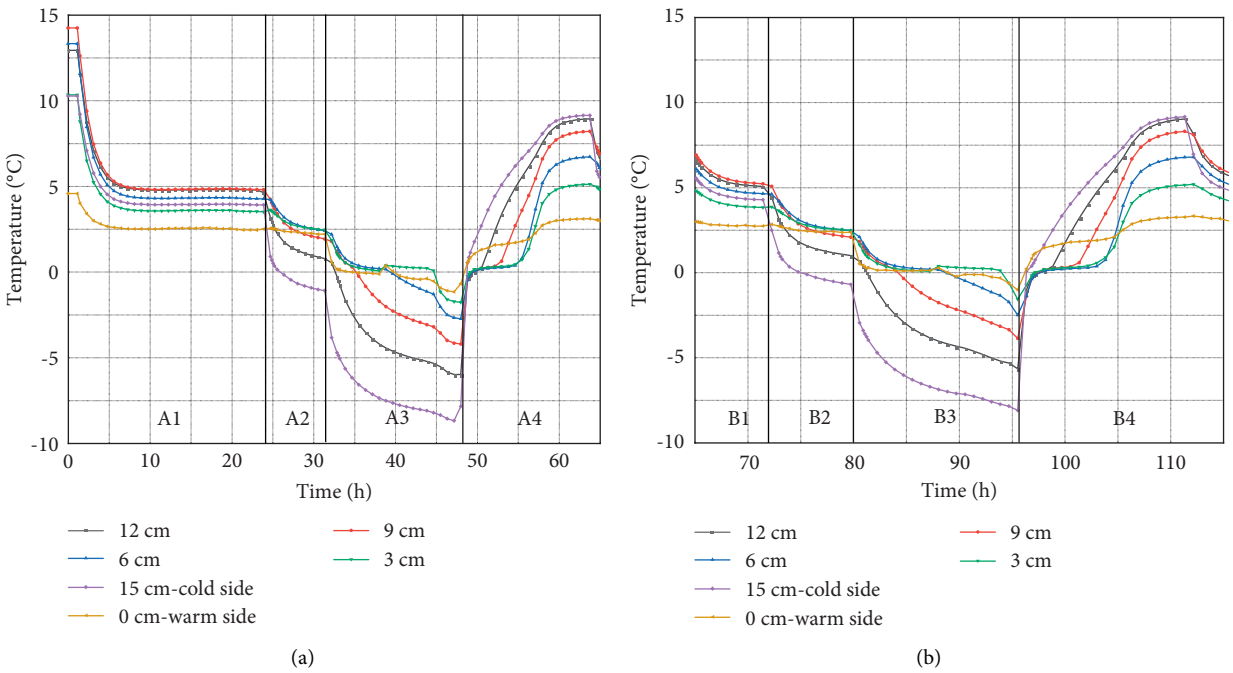

(a) (b)

Figure 7: Temperature history: (a) the first constant temperature, freezing, and thawing; (b) the second constant temperature, freezing, and thawing.

pressure generated after freezing. The duration and degree of this stage are determined by the properties of the graded sand and the freezing gradient, as well as the number of cycles.

3.4. Water Supply and Water Refill Rate. As shown in Figure 10(a), the water supply switch for graded sand was not opened, and 2.5 ml moisture fluctuation was the final adjustment stage of the instrument at location A1. The water supply was then stable and slow, and the analysis revealed that there was slow air pressure leakage at the interface. In the A2 stage, as the freezing temperature is applied, the sand test begins to freeze, and the Markov water bottle quickly replenishes water and then gradually stabilizes. In the A3 stage, the water supply switch is closed. In the A4 phase, as the temperature rises, the graded sand samples begin to replenish water quickly. The rate of filling water gradually becomes constant, and no water replenishment reaches a stable state. As shown in Figure 10, the amount of filling water is approximately 19 mL.

At the B1 stage, the graded sand soil is slowly refilled with water at a low rate when the sample is constant. As the freezing temperature is applied in the B2 phase, the graded sand samples begin to replenish water, but the rate drops quickly. In stage B3, the water supply switch is closed. As the temperature rises at the B4 stage, the graded sand quickly begins to replenish water, and the replenishing rate gradually

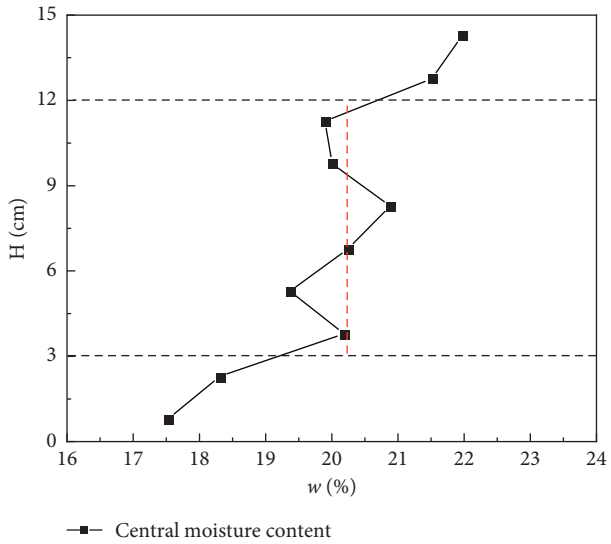

Figure 8: Water content distribution.

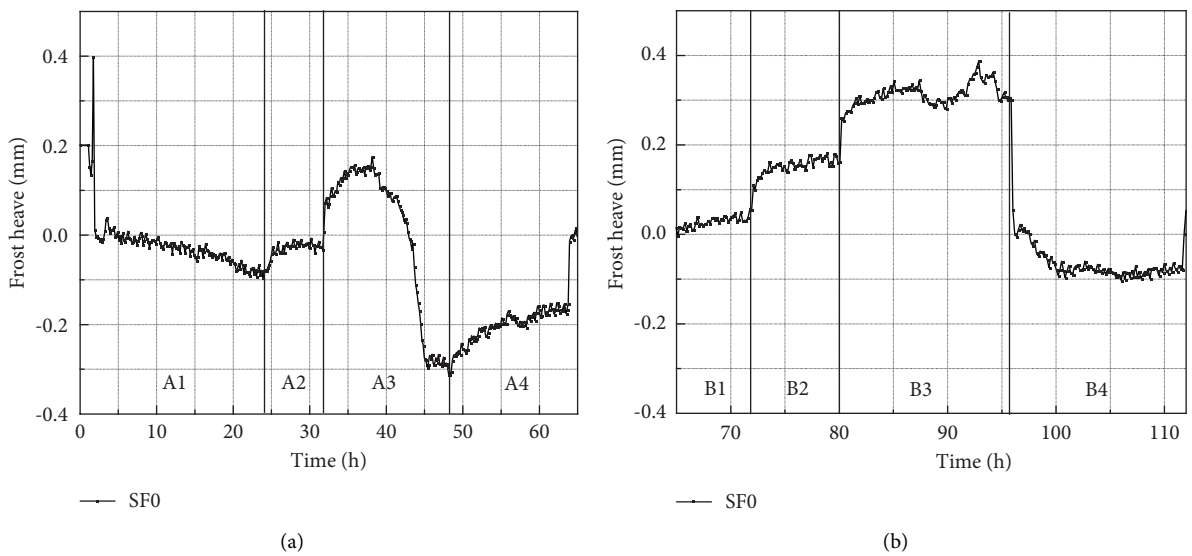

Figure 9: Development of frost heave under free-thaw cycles: (a) the first cycle; (b) the second cycle.

becomes constant, reaching a stable state without filling water, and the replenishment amount is approximately 24 ml.

By comparing Figures 10(a) and 10(b), the number of freeze-thaw cycles leads to increased water replenishment for graded sand. According to the analysis, the number of freeze-thaw cycles increases the water migration capacity of intermediate sand during the freezing process, increasing water replenishment. In conclusion, although graded sand has little frost heave, the phenomenon of frost heave also occurs with the rise of freeze-thaw cycles. As a result, freezing damage to graded coarse-grained soil is caused not by frost heaving deformation but by a decrease in soil structure and strength due to hydrothermal coupling and an increase in soil deformation due to thawing load action.

4. Validation of the Numerical Model

4.1. Model Validation One. This paper used the secondary development function PDE module of numerical software COMSOL Multiphysics to establish the column model. The software simulated the SF0 graded sand test. The difficult results in [21] were compared and analyzed. The input parameters of the model are shown in Table 3. The width of the soil is 0.05 m, and the height is 0.2 m. The initial temperature field at the cold end was +1°C, and the initial temperature at the warm end was +4°C. The sample was kept constant for 24 h. After constant temperature, the soil samples were frozen at a steady rate of about 1.5°C/day at the cold end for about 320 h. The boundary is used to set water refill boundary conditions. The calculation time of the model

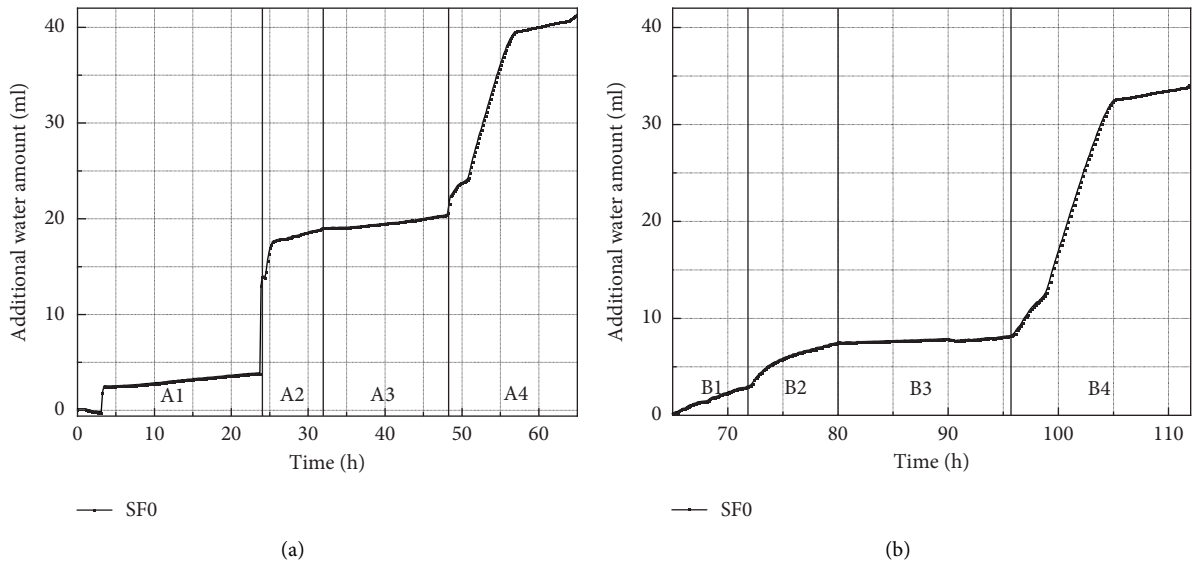

Figure 10: Replenishment distribution: (a) the first constant temperature is freezing and thawing; (b) the second is freezing and thawing.

Table 3: Model input parameters.

Test	Thermal conductivity of soil particles λ_s (W/(m·°C)	Thermal conductivity of water λ_w (W/(m·°C))	Thermal conductivity of ice λ_i (W/(m·°C))	Heat capacity of soil particles C_S (J/(kg °C)	Heat capacity of water C_W (J/(kg °C)	Heat capacity of ice C_i (J/(kg °C)	Soil saturated infiltration coefficient K_s (m/s)
SF0	1.46	0.57	2.26	900	4180	2100	4×10^{-7}
Konrad	2.58	0.57	2.26	900	4180	2100	2.12×10^{-6}

is 344 hours, consistent with the test conditions, and the calculation step is one hour.

Figure 11 shows the time-varying curves of the measured and simulated temperature values at the height of the SF0 soil column in graded sand at 6 cm, 9 cm, and 12 cm. The measured temperature values are consistent with the simulated values calculated by the model. However, there are still minor errors in the initial and other periods. The analysis shows that due to the variability of instruments and environmental factors during the test, the temperature of the soil after constant temperature does not reach a uniform temperature, resulting in a deviation from the initial temperature of the Earth simulated by numerical simulation.

Figure 12 compares the test and simulation values of water content at different heights with the curve of soil height. Due to mutual water migration in the soil during freezing, closely related to the number of freeze-thaw cycles, the simulation only simulated the moisture content after the first freezing without considering the freeze-thaw process. Therefore, there will be some errors between the water content results and the simulated values after two freeze-thaw cycles. Still, the variation trend of water content with soil height after water migration is the same.

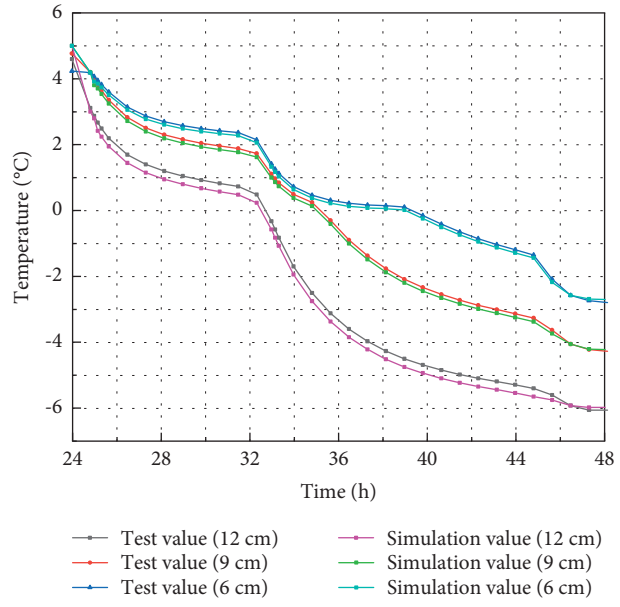

Figure 11: Comparison of temperature calculation results and test results.

4.2. Model Validation Two. The characteristics of the temperature field distribution of specimen F10K50 and the moisture distribution of model F5K50 after freeze-thaw cycles are given in the literature [21] (FxKy, x denotes the percentage of fine content, and y represents the percentage of kaolin content in the penalties). These are shown in Figure 13 and Figure 14.

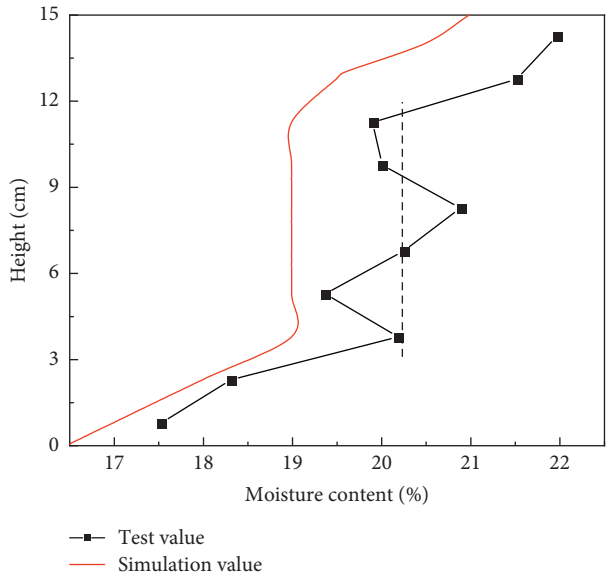

Figure 12: Comparison of water content calculation results and test results.

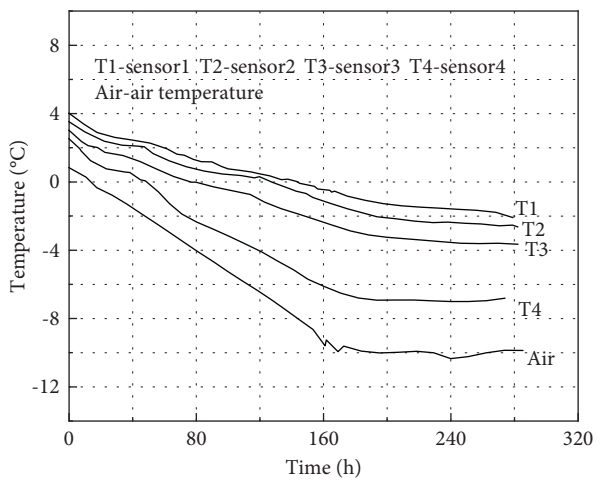

Figure 13: Temperature distribution of F10K50 sample.

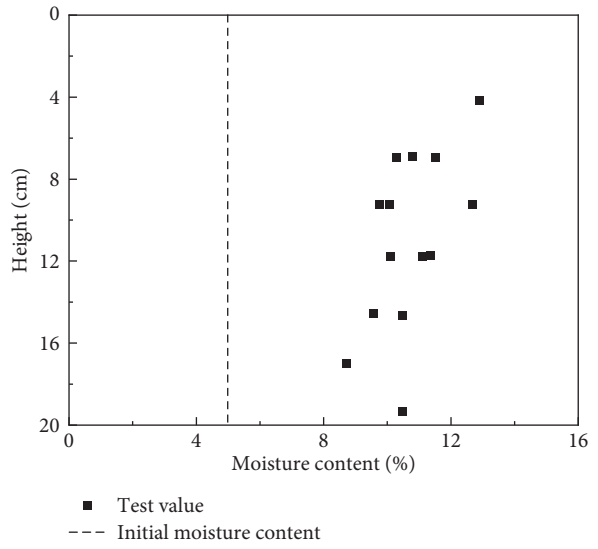

Figure 14: Water distribution of F5K50 sample.

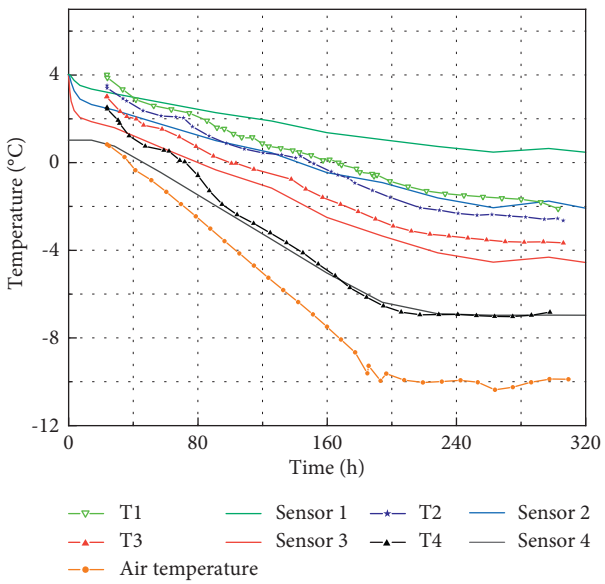

Figure 15: Comparison of simulated and experimental values of temperature.

The temperature field distribution of F10K50 was obtained by numerical simulation of hydrothermal coupling, and the numerical simulation temperature distribution and the experimental temperature distribution are shown in Figure 15. As can be seen from the figure, the first 24 h is the constant temperature phase of the test, and the temperature distribution of each simulation point is the same as the test temperature, except for the warm end. After the cooling process starts, the closer the cold end gets, the greater the cooling rate. During the test, the cooling of the cold end affected the reduction of the ambient temperature, which led to the actual temperature of the warm end being much lower than +4°C. But the overall temperature field distribution can verify the correctness and validity of the model.

The moisture field distribution of F5K50 specimens frozen for the first time under the same conditions was obtained by numerical simulation of hydrothermal coupling. The moisture distribution was calculated by numerical simulation, and the moisture distribution after experimental freeze-thaw cycles is shown in Figure 16. As can be seen from the figure, under the open system, a significant increase in the water content of the soil column occurred from the initial 5%, especially in the upper 6 cm, where necessary freezing and water absorption occurred. Since the effect of freeze-thaw cycles is not considered in the hydrothermal-coupled calculation model, the moisture distribution after the first and after the fourth freezing will change somewhat even under the same conditions. Therefore, there will be some errors between the experimental and simulated water content values, but their trends are the same. In summary, the literature proved the rationality and correctness of this hydrothermal coupling calculation model by simulating the temperature and moisture fields of two specimens, F10K50 and F5K50.

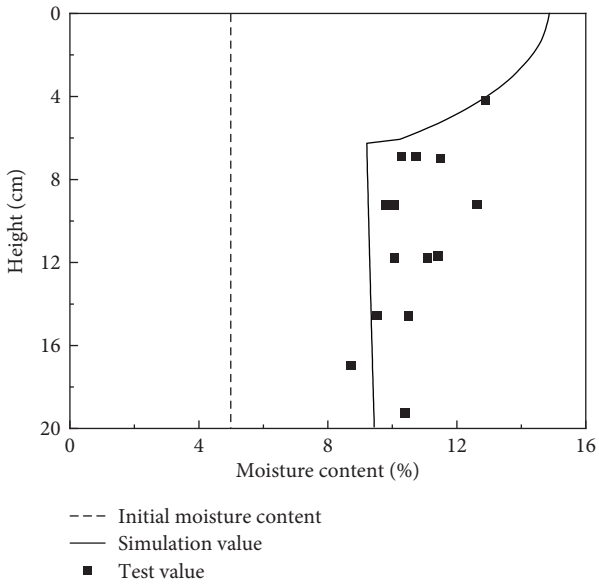

Figure 16: Comparison of simulated and experimental values of water.

5. Conclusions

In this study, Harbin Songhua River sand and 1,250 mesh fine ground kaolin were used as samples, and four types of fine sand with 0%, 5%, 10%, and 15% fine-grained content were configured. Particle analysis and compaction tests were conducted. Finally, the unidirectional freezing test of graded sand with zero fine-grain content was performed. The following is a summary of the findings:

(1) With the increase of fine-grain content, the maximum dry density of fine sand increases gradually, and the change interval of dry density in the experiment also increases slowly.

(2) The temperature gradient and the number of freeze-thaw cycles considerably affect the freezing process of graded sands. The greater the temperature gradient, the more freeze-thaw cycles there are and the greater the frost heave.

(3) The graded sand with zero fine particle content has obvious freezing shrinkage and thaw settlement during the freezing process. The changing trend of its frost heave corresponds roughly to the four developmental stages. However, generally, the frost heave of graded sands is small, and the frost heaving rate is low. Frost damage is not owing to frost heaving deformation but to the coupling of water and heat, which damages the soil structure and greatly reduces bearing capacity.

Finally, due to the epidemic, only one group of the unidirectional freezing tests was completed. Subsequently, one-way freezing tests can be carried out on graded sand soils with different fine content to obtain more test data for comparative analysis and to study the influence of good content on the freezing process of graded sand soils. However, the paper's findings can provide a reference for the engineering design and application of graded coarse-grained soil fill in cold regions.

Data Availability

The data used to support the findings of this study are included within the article.

Conflicts of Interest

The authors declare that they have no conflicts of interest.

Acknowledgments

The authors thank the workers, foremen, and safety coordinators of the main contractors for their participation. This research was supported by the National Natural Science Foundation of China (Grant nos. 42101125 and 41772315).

References

[1] L. J. Qi and W. Ma, "State-of-art of research on mechanical properties of frozen soils," *Rock and Soil Mechanics*, vol. 1, pp. 133–143, 2010.

[2] S. B. Huang, Q. S. Liu, A. P. Cheng, Y. Liu, and G. Liu, "A fully coupled thermo-hydro-mechanical model including the determination of coupling parameters for freezing rock," *International Journal of Rock Mechanics and Mining Sciences*, vol. 103, pp. 205–214, 2018.

[3] R. Zhu, Z. Y. Cai, Y. H. Huang, C. Zhang, W. Guo, and Y. Wang, "Effects of wetting-drying-freezing-thawing cycles on mechanical behaviors of expansive soil," *Cold Regions Science and Technology*, vol. 193, Article ID 103422, 2022.

[4] S. Y. Li, M. Y. Zhang, W. S. Pei, and Y. Lai, "Experimental and numerical simulations on heat-water-mechanics interaction mechanism in a freezing soil," *Applied Thermal Engineering*, vol. 132, pp. 209–220, 2018.

[5] B. Li, Z. W. Zhu, J. G. Ning, T. Li, and Z. Zhou, "Viscoelastic–plastic constitutive model with damage of frozen soil under impact loading and freeze–thaw loading," *International Journal of Mechanical Sciences*, vol. 214, Article ID 106890, 2022.

[6] D. H. Everett, "The thermodynamics of frost damage to porous solids," *Transactions of the Faraday Society*, vol. 57, pp. 1541–1551, 1961.

[7] F. Z. Tong, L. Gao, X. P. Cai, Y. Zhong, W. Zhao, and Y. Huang, "Experimental and theoretical determination of the frost-heave cracking law and the crack propagation criterion of slab track with water in the crack," *Applied Sciences*, vol. 9, no. 21, p. 4592, 2019.

[8] Z. H. Cheng and Y. S. Deng, "Bearing characteristics of moso bamboo micropile-composite soil nailing system in soft soil areas," *Advances in Materials Science and Engineering*, vol. 2020, Article ID 3204285, 2020.

[9] H. Wang, Y. K. Wu, M. Wang, and G. Li, "Influence of fines content and degree of saturation on the freezing deformation characteristics of unsaturated soils," *Cold Regions Science and Technology*, vol. 201, Article ID 103610, 2022.

[10] L. Geng, S. Y. Cong, J. Luo, X. Ling, X. Du, and Y. Yu, "Stress–strain model for freezing silty clay under frost heave based on modified takashi's equation," *Applied Sciences*, vol. 10, no. 21, p. 7753, 2020.

[11] L. Tang, Z. H. Cheng, X. Z. Ling, S. Cong, and J. Nan, "Preparation and performance of graphene oxide/self-healing microcapsule composite mortar," *Smart Materials and Structures*, vol. 31, no. 2, Article ID 025022, 2022.

[12] X. Z. Ling, J. Luo, and L. Geng, "Coupled hydro-thermo-deformation frost heave model for unsaturated expansive soils in seasonally frozen soil regions," *Chinese Journal of Geotechnical Engineering*, vol. 7, pp. 1255–1265, 2022.

[13] T. L. Wang and Z. R. Yue, "Influence of fines content on frost heaving properties of coarse-grained soil," *Rock and Soil Mechanics*, vol. 34, no. 2, pp. 359–365, 2013.

[14] J. L. Ju, "Experiment and study on frozen heave factor of soil," *Journal of Water Resources and Architectural Engineering*, vol. 2, no. 2, pp. 51–54, 2004.

[15] M. Guo, X. Ren, and Y. B. Jiao, "Review of aging and antiaging of asphalt and asphalt mixtures," *China Journal of Highway and Transport*, vol. 4, pp. 41–59, 2022.

[16] Y. J. Jiang, "Frost heave performance of graded coarse-grained soil considering fine particle content," Ph.D. thesis, Harbin Institute of Technology, Harbin, 2020.

[17] Y. S. Deng, Z. Cheng, M. Z. Cai, Y. Sun, and C. Peng, "An experimental study on the ecological support model of dentate row piles," *Advances in Materials Science and Engineering*, vol. 2020, Article ID 6428032, 2020.

[18] H. Su, Y. J. Hang, Y. S. Song, K. Mao, D. Wu, and X. Qiu, "Seismic response of anchor+hinged block ecological slope by shaking table tests," *Advances in Materials Science and Engineering*, vol. 2018, Article ID 7684831, 2018.

[19] C. W. Yang, J. J. Zhang, Q. Honglue, B. Junwei, and L. Feicheng, "Seismic earth pressures of retaining wall from large shaking table tests," *Advances in Materials Science and Engineering*, vol. 2015, Article ID 836503, 2015.

[20] X. S. Liu, W. Guo, J. Z. Li, and H. Zhang, "Seismic study of skew bridge supported on laminated-rubber bearings," *Advances in Civil Engineering*, vol. 2020, Article ID 8899693, 2020.

[21] J. M. Konrad and N. Lemieux, "Influence of fines on frost heave characteristics of a well-graded base-course material," *Canadian Geotechnical Journal*, vol. 42, no. 2, pp. 515–527, 2005.